Effects of spreading widths upon the direct nuclear reaction continuum*

M. B. Lewis
Oak Ridge National Laboratory, Oak Ridge, Tennessee 37830
(Received 5 August 1974)

Simple concepts which can be directly applied to measurements of resonances and the accompanying continua have been studied. Pickup reaction spectra leading to hole states in the continuum were found to give an understanding of the excitation energy dependence of resonance damping and the concurrent rise of "background" continuum states. When these hole resonances are parametrized in terms of the shell model, they can be used to predict the energy dependence of the damping of more complex resonances, such as collective particle-hole excitations in the inelastic scattering spectra. Furthermore, it is proposed that part of the background continuum in pickup spectra is the semidirect excitation of the 2h-1p states, the density of which determines both the nuclear damping width and the continuum cross section.

[NUCLEAR REACTIONS ^{208}Pb(^{3}He, α), $E = 75$ MeV, ^{209}Bi(p, d), $E = 62$ MeV; calculated continuum cross sections in a direct reaction.]

I. INTRODUCTION

In recent publications two new aspects of direct nuclear reaction spectra have come to light. First,[1] a study of the ^{120}Sn(p, d) reaction at $E_p = 57$ MeV has shown that deep-lying hole states in the nuclear continuum of medium-weight nuclei are sufficiently "narrow" ($\Gamma \approx 4$ MeV) that they can be directly measured. Second,[2] a study of the (p, p') reaction at $E_p = 62$ MeV, as well as other scattering reactions, has shown that high-energy collective excitations (probably strong quadrupole excitations) can be directly observed in the nuclear reaction continuum. From the viewpoint of nuclear spectroscopy, these observations may be said to complement well-established properties of low-lying discrete states of the nucleus. For example, we know that the ^{120}Sn(p, d) reaction preferentially excites the states $3s_{1/2}$, $2d_{3/2}$, $1h_{11/2}$, $2d_{5/2}$, and $g_{7/2}$ in the $N = 50$–82 valence shell so that the new observation[1] of the $g_{9/2}$ hole in the $N = 28$–50 inner shell represents the complement of expected sum rule strength for deep-lying hole states in ^{119}Sn. In the case of collective quadrupole excitations, only 10–20% of the energy-weighted sum rule strength is exhausted by low-lying discrete states in nuclei[3]; thus, the observation of a strong collective quadrupole resonance in the continuum is again the spectroscopic complement of the bound states and a fulfillment of well-known sum rules. However, the resonances in a direct reaction continuum are generally difficult to observe. This results from the fact that the resonances are broad and coexist with a large reaction background continuum. In this paper, we will attempt to understand more quantitatively the degree of spreading of spectroscopic strength and the formation of a background continuum.

The general features of a reaction spectrum at moderate bombarding energies (≈100 MeV) is schematically illustrated in Fig. 1. With typical particle resolution (≲100 keV), the spectrum can be dissected into discrete, continuum, and evaporation components. It is useful in the discussions that follow to make a further qualitative dissection of the continuum into two components. The low excitation (E_x) region of the continuum will be referred to as the direct reaction continuum (DRC) region, while the low particle-energy (E_b) region will be the equilibrium region of the continuum. Each region is typically characterized by a pronounced variation in the cross section $\sigma(E_b)$. In the DRC region, the variation is due to "giant" resonances in the general sense, i.e., further depletion of the same sum rules which applied to the discrete region [for example, the excitation of deep-lying hole states as discussed in the ^{120}Sn-(p, d) reaction above]. In the equilibrium region of the continuum, the variation (if not suppressed by Coulomb effects) is an accumulation of low-energy particles from the (complete or incomplete) thermalization and evaporation of the nucleus.

The study of the lower particle-energy region of the continuum is sometimes referred to as the "precompound" or "preequilibrium" region.[4] In the preequilibrium model the incident projectile energy is dissipated through the compound system by the generation of successively more complex states of the projectile-plus-target system (e.g., 1p → 2p-1h → 3p-2h → ··· to equilibrium). The treatment is statistical, and the direct angular momentum transfer is not calculated. These approximations are reasonable for the low (particle) energy region of the continuum, but not reasonable for

the higher (particle) energy region where nuclear structure could be important and where the angular distribution $[\sigma(\theta)]$ of the nonresonant continuum is not isotropic or even symmetric about 90°.

In the following discussion, we show more specifically the various quantitative aspects of the DRC region of the nuclear reaction spectrum. We propose that the continuum cross section in the DRC region can be estimated by the Born-approximation approach in which most of the specific angular momentum effects are taken into account by the usual partial wave expansion. Although this approach to continuum phenomena is meant to be a general one, we focus our attention upon the neutron pickup reaction since the basic principles are most simply illustrated and the relevant data have been published.

II. GENERAL FEATURES OF THE PICKUP REACTION

A. ^{208}Pb(^{3}He, α)^{207}Pb reaction at $E_{He} = 75$ MeV

A forward-angle reaction spectrum (for $E_x < 14$ MeV) is shown in Fig. 2. These data[5] were taken with a solid-state counter telescope with energy resolution ≈200 keV so that various particles in the reaction could be distinguished. The authors made special efforts in the experiment to exclude from the data possible spurious effects due to slit scattering, target impurities, etc. The spectrum in Fig. 2 is plotted in 0.5-MeV bins for convenience and the "peaks" for excitation below 4 MeV are merely sketched in, since they have already been studied in detail in a previous work[6] at slightly lower bombarding energy. The peaks essentially exhaust the available sum rule strength for the $N = 82-126$ valence shell. The cross section strength for $E_x > 4$ MeV may be due in part to the excitation of more deeply lying (inner shell) hole states.

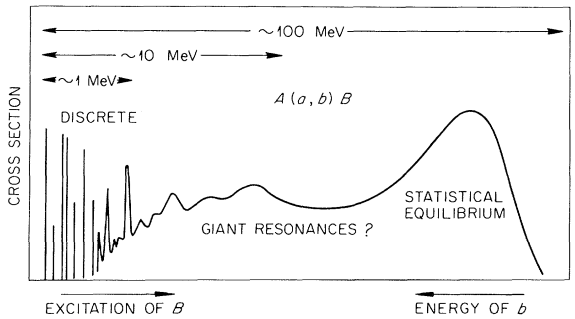

FIG. 1. Schematic illustration of the various regions of a typical reaction spectrum taken at medium bombarding energies.

In Fig. 3 the quasidiscrete region of Fig. 2 is enhanced by expanding the cross section scale and contracting the energy scale. Uncertainties are given in Ref. 5. It is clear from Fig. 3 that the enhanced region of the continuum is finite in extent ($E_x \lesssim 20$ MeV) so that it may be possible to distinguish between resonant and nonresonant components of the continuum. Another feature of Fig. 3 is that the enhanced region is not symmetric but manifests an extended high excitation tail. A further property of the resonance is that it is seen only in the spectra at forward angles where direct reaction amplitudes are expected to be large.

The above remarks imply that at least two reaction mechanisms are pertinent to the spectrum: (1) the direct reaction which accounts for the discrete states and the enhanced region of the continuum and (2) the indirect reaction which explains the large "background" under the resonance and at "excitation" energies beyond the resonance (i.e., $E_x \gtrsim 20$ MeV). While we assume that the direct component can be estimated by the usual distorted-wave Born approximation (DWBA), it is less clear how to understand the indirect component. It can be seen in Fig. 3 that, while the direct component appears to become damped out in the region $E_x \approx 10-20$ MeV, the indirect component, which was

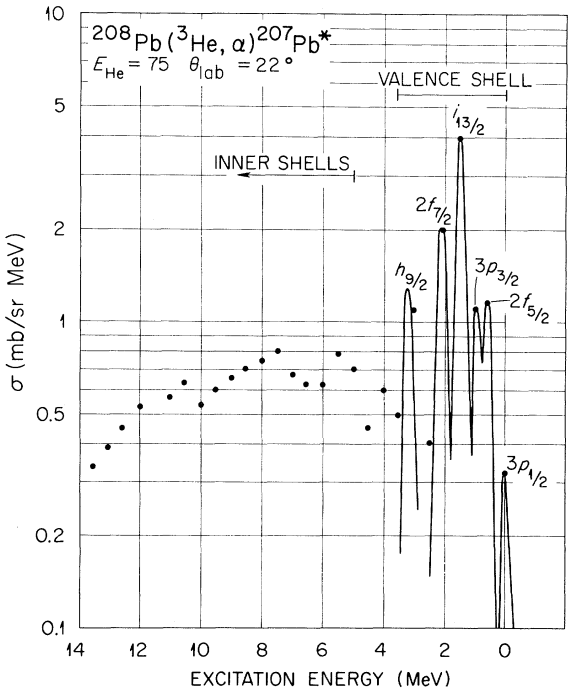

FIG. 2. Spectrum of the ^{208}Pb(τ, α) reaction. Data are from Ref. 5. Neutron hole states in the $N = 82-126$ shell are identified as the valence shell while the broad resonance structure above 5 MeV includes inner shell states.

negligible in the low excitation or discrete region, apparently increases so as to compensate partially the continuum cross section. This fact suggests a correlation between the mechanism which damps or broadens the resonant hole state and that which generates the nonresonant continuum.

B. Damping mechanism for the resonance

In the shell or particle-hole model of nuclear states, it is clear that a single particle or hole with sufficiently high energy will be nearly degenerate with a more complex configuration composed of particles and holes of lesser energy.[7] The implication of this condition for inner shell-hole states is given in Fig. 4. The hole state at $E \approx 6$ MeV could be nearly degenerate with various 2h-1p states (center of Fig. 4) since the neutron shell gap in ^{208}Pb($N = 126$) is only about 3 MeV. Furthermore, the density of such 2h-1p states must increase rapidly with increasing excitation energy (discussed below). Many of the 2h-1p levels in the quasidiscrete continuum are particle unbound (the neutron threshold for ^{207}Pb is 6.7 MeV). However, the centrifugal barrier for the unbound particle,

$$\frac{\hbar^2}{2Mr^2} l(l+1) \approx 21 \frac{l(l+1)}{r^2} \text{ MeV} , \tag{1}$$

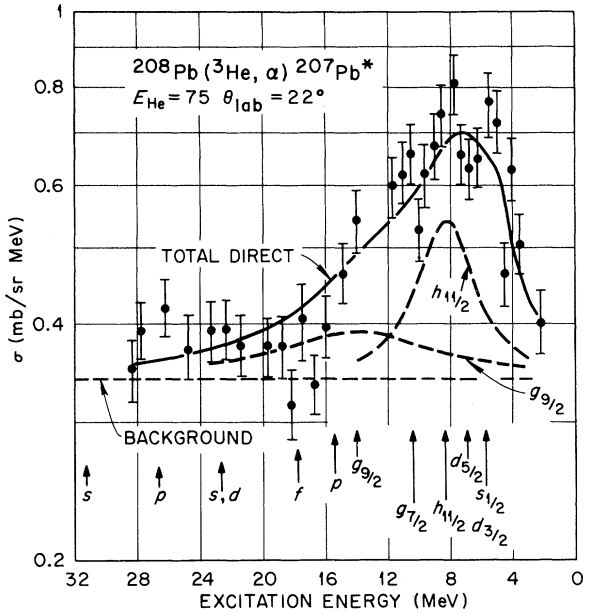

FIG. 3. Details of the inner shell region of Fig. 2. Data and uncertainties are from Ref. 5. The solid curve is a prediction for direct reaction pickup from inner shell states while the background represents indirect reaction mechanisms. Examples of the $1h_{11/2}^{-1}$ and $1g_{9/2}$ components are shown, and the positions of other $N < 82$ states are indicated.

where $r \approx$ nuclear radius (in fm), is several MeV for most particle orbits ($l > 1$) so that particle penetrabilities are generally small.[8]

It is not the purpose of this work to make detailed calculations of level densities or widths. However, the expected trends of these quantities can be brought to light by using statistical approximations. For example, if it is assumed that the single-particle levels are equally spaced in the nucleus (equidistant spacing model) with density, g levels/MeV, then the density of 2h-1p levels is given[9] by

$$\rho(E) \tfrac{1}{4} g^3 E^2 , \tag{2}$$

where E is the excitation energy of the system. As a result of the near energy degeneracy between the initial hole state and some of the 2h-1p spectrum of levels of density ρ, the hole state can readily decay into (or mix with) the 2h-1p continuum. This "thermalization" of the hole energy is indicated by the lower diagram in Fig. 4. The average decay rate is given by first-order perturbation theory, with a width (in MeV) of

$$\Gamma = 2\pi \langle M^2 \rangle \rho(E) , \tag{3}$$

where $\langle M^2 \rangle$ is the average squared matrix element in the 1h-2p transition. These matrix elements are equivalent (by crossing relations[10]) to the more familiar two-body matrix elements used in shell model calculations in the lead region. Consequently, the "spreading width" of a hole

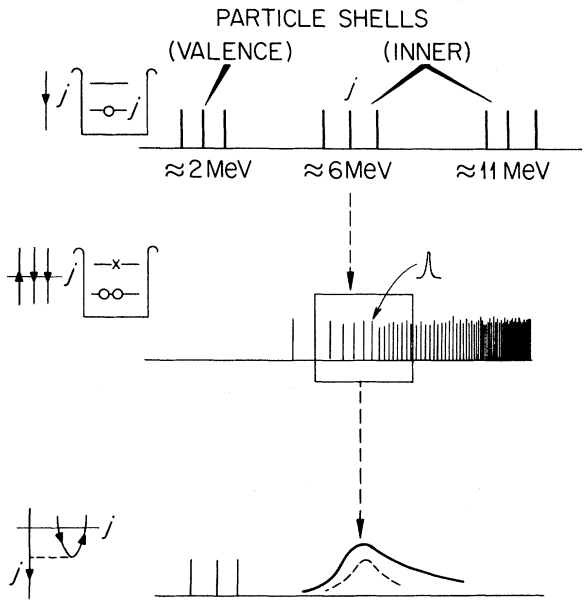

FIG. 4. Schematic illustration of the damping or spreading of the inner shell hole strength (top of figure) into the 2h-1p "sea" of levels (middle of figure) by the inelastic scattering of the hole state (bottom of figure).

state can be estimated using parameters g and M, which we already know approximately. From Eq. (2) and (3)

$$\Gamma \simeq s'E^2, \text{ with } s' = \tfrac{1}{2}\pi g^3 \langle M^2 \rangle \ . \tag{4a}$$

The s will be referred to as the spreading parameter. In the scattering diagram in Fig. 4, the particle-hole excitation may take place in either the neutron or proton shell. Thus $s' \to s'_p + s'_n \approx 2s'$ or

$$\Gamma \approx sE^2 \text{ with } s = \pi g^3 \langle M^2 \rangle \ , \tag{4b}$$

where the matrix element is averaged over both neutrons and protons.

We have referred to the 2h-1p states independently of their total angular momentum and parity which must be the same as the j^π of the hole state. However, it can be demonstrated that for any particular (2h-1p)J^π configuration, the possibility of coupling to $J=j$ is nearly assured. The parity of the final $2h_f$-$1p_f$ configuration is usually the same as the parity of the initial $1h_i$ state since the two holes, $2h_f$, are typically in the same major shell ($\pi_{2h_f} = +$), while the $1p_f$ is two major shells from the h_i and therefore has usually the same parity ($\pi_{p_f} = \pi_{h_i}$). This argument is less secure at very high excitation energies, and the spreading widths become slightly overestimated.

C. Incorporation of the direct reaction (DWBA)

Although the mixing or damping of the hole state into the 2h-1p continuum modifies the shape of the reaction spectrum, the sum rules and the validity of the direct reaction theory are expected to remain the same for the resonant part of the quasi-discrete continuum. Thus, we assume for the general shape of this part of the continuum,

$$\sigma(E, \theta) = \sigma^{(1)}(\theta, E) + \sigma^{(2)}(\theta, E) + \cdots \ , \tag{5}$$

where $\sigma^{(1)}(\theta, E)$ is the direct excitation of the giant resonances. The simple addition of a nondirect term $\sigma^{(2)}(\theta, E)$ implies the incoherent addition of direct and nondirect reaction amplitudes. The approximation follows from the fact that the nonresonant term $\sigma^{(2)}(\theta, E)$ is derived from many states of various spin and parity, all but one J^π of which is different from that of the resonance.

The direct term is given by the usual resonance form,

$$\sigma^{(1)}(\theta, E) = \sum_j \frac{\Gamma_j^f(\theta)\Gamma_j^d/2\pi}{(E - E_j)^2 + (\Gamma_j^d/2)^2} = \sum_j \Gamma_j^f(\theta) R(E, E_j) \ , \tag{6}$$

where the sum is over the hole states j. This resonant term is normalized to preserve the usual shell model sum rules:

$$\int_0^\infty \sigma^{(1)}(\theta, E) dE = \sum_j \Gamma_j^f(\theta) \int_0^\infty R(EE_j) dE = \sum_j \Gamma_j^f(\theta) \ ,$$

where $\Gamma_j^f(\theta) = S_j \sigma_j^{\mathrm{DW}}(\theta)$ is the formation probability of the state with energy E_j and might be determined by the product of the spectroscopic factor S_j and the DWBA differential cross section, $\sigma_j^{\mathrm{DW}}(\theta)$, for particle or hole state j. In general, all the sum rule strength is assumed to be located in the resonance region so that we take $S_j = 2j + 1$, the full occupancy of the shell model orbit; $\Gamma_j^d = \Gamma^d(E_j)$ is the decay or spreading width of a hole state j as discussed in Sec. II B.

D. Semidirect reaction components

The second term, $\sigma^{(2)}(\theta, E)$, in Eq. (5) represents a semidirect (e.g., two-step) reaction cross section, the magnitude of which is not governed by the sum rules in Sec. II C. It is reasonable to assume that the 2h-1p states themselves can be excited in other ways also. The mechanism would be a two-step process; i.e., particle-hole excita-

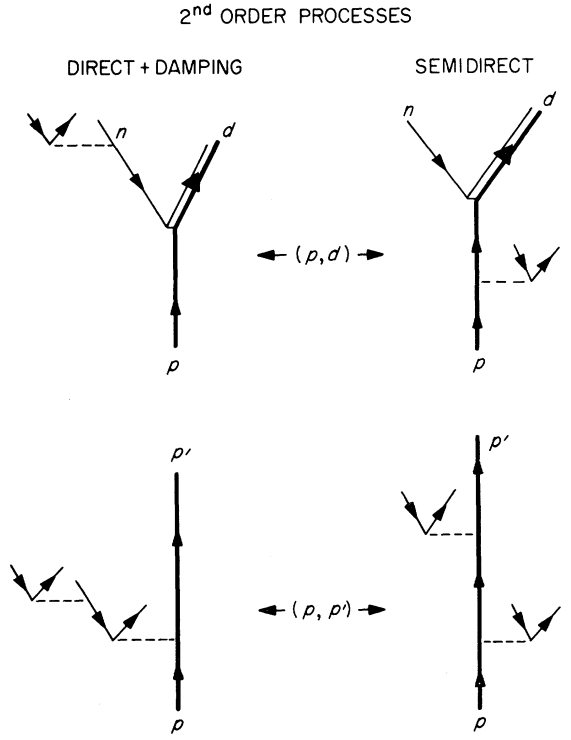

FIG. 5. Scattering diagrams for second-order processes—direct reaction followed by damping, and two-step (semidirect reaction) mechanisms in the (p, d) and (p, p') reactions initiated by medium energy projectiles (heavy lines).

tion followed by, or following, pickup as shown in the diagram in Fig. 5. This two-step process would be analogous to the one-step plus damping process discussed above (i.e., second order). Although the excitation probability of any one of these more complex states is much smaller than the direct excitation of the hole states, the level density is much larger. Furthermore, since the level density of 2h-1p states increases as a function of excitation energy, the damping of the hole strength will become more severe while the total excitation of the 2h-1p components will increase. Thus, the decrease in $\sigma^{(1)}(\theta, E)$ is qualitatively compensated by an increase in $\sigma^{(2)}(\theta, E)$ which tends to make the continuum more uniform in energy, in agreement with experimental results.

To illustrate how the semidirect reaction continuum might be calculated, let us assume we have estimated the cross section $\sigma_i'(\theta, E_i')$ for the two-step (e.g., inelastic scattering plus pickup) excitation in which a 2h-1p state (i) is excited with excitation energy region E_i at scattering angle θ.

We now proceed to apply the same statistical formalism to the damping width Γ of these states with density ρ as in the case of the hole states in Sec, II C. The equivalent of Eq. (6) becomes

$$\sigma^{(2)}(\theta, E) = \sum_i \sigma_i'(\theta, E_i) R(E, E_i) \ . \tag{7a}$$

In the continuum this becomes

$$\sigma^{(2)}(\theta, E) = \int \langle \sigma'(\theta, E') \rangle R(E, E') \rho(E') dE' \ . \tag{7b}$$

Or, for convenience of the computation for the reaction $A(a, b)B$,

$$\sigma^{(2)}(\theta, E) \approx \langle \sigma'(\theta) \rangle \int (k_b/k_a)^{1/2} R(E, E') \rho(E') dE' \ , \tag{7c}$$

where the usual phase-space (momentum) dependence $(k_b/k_a)^{1/2}$ on the reaction cross section is shown explicitly, and the remaining cross section has been averaged over various 2h-1p final state configurations. The integration range is over the excitation region of the nucleus B. The approximation [Eq. (7c)] is valid only in the E_b energy range where Coulomb and angular momentum barrier effects are small, i.e., in the lower excitation (higher E_b) energy region of the continuum. In this paper we are only interested in the excitation region $E_x \lesssim 30$ MeV.

TABLE I. Shell model ($N \leq 126$) states for neutrons in ^{208}Pb. Col. 1: configuration; col. 2: calculated excitation from Ref. 11; col. 3: measured energies from Ref. 6; col. 4: energies assumed in this work to estimate continuum resonance structure; col. 5: level widths calculated assuming E_j in col. 4.

nlj	E_{calc} (MeV)	E_{meas} (MeV)	E_j (MeV)	Γ_j^d (MeV) $s = 0.05$ MeV^{-1}
$3p_{1/2}$	0.6	0.0	···	···
$2f_{5/2}$	1.7	0.6	···	···
$3p_{3/2}$	1.5	0.9	···	···
$1i_{13/2}$	3.4	1.6	···	···
$2f_{7/2}$	4.2	2.3	···	···
$1h_{9/2}$	4.8	3.4	···	···
$3s_{1/2}$	8.9	···	5.7	1.8
$2d_{3/2}$	9.2	···	5.7	1.8
$1h_{11/2}$	9.9	···	8.3 ± 1.0	3.7
$2d_{5/2}$	11.0	···	6.8	2.5
$1g_{7/2}$	12.1	···	10.7	5.8
$1g_{9/2}$	15.7	···	14	10
$2p_{1/2}$	16.2	···	15	11
$2p_{3/2}$	17.3	···	16	13
$1f_{5/2}$	18.7	···	17	14
$1f_{7/2}$	21.0	···	19	18
$2s_{1/2}$	23.1	···	23	26
$1d_{3/2}$	24.5	···	25	31
$1d_{5/2}$	25.7	···	26	34
$1p_{1/2}$	29.3	···	29	42
$1p_{3/2}$	29.9	···	30	45
$1s_{1/2}$	33.3	···	33	54

III. APPLICATION OF THE MODEL TO PICKUP REACTIONS

A. Resonance region

In order to apply the above prescription to the measurements of the continuum spectra in a pickup reaction, it is first necessary to know the approximate locations or separation energies for deeply lying particle shells. We chose for these energies those recently estimated by Cusson, Kolb, and Trivedi,[11] since these predictions give binding energies for the valence shells in reasonable agreement with experiment. These values are given in Table I. The $3p_{1/2}$ to $1h_{9/2}$ shells are the valence shells which give rise to the well-known discrete hole states in ^{207}Pb. Thus, what we refer to as inner shell states which give rise to the resonances in the quasidiscrete continuum begin with the $3s_{1/2}$ shell, i.e., $E_{\text{calc}} = 8.9$ MeV.

However, it is clear from Fig. 2 and the (p, d) spectra discussed below that the calculated energies (E_{calc}) are slightly too high to explain the threshold ($E_x \approx 5$ MeV) of the inner shell resonance. Thus, we have assumed slightly lower energies E_j for the inner shell states as shown in Table I. The reduced direct reaction cross sections, $\sigma_j^{\text{DW}}(\theta)$, were computed with the code[12]

DWUCK; the optical model parameters for the ^{3}He, α, p, and d used are from Refs. 6, 13–15. The spreading parameter could then be adjusted to reproduce the over-all shape of the resonances in both the (^{3}He, α) and (p, d) spectra. Finally, a background continuum representing the indirect reaction components was determined as the difference between the total measured cross section and the prediction for the direct component.

The results of these calculations are given by the curves in Fig. 3 for (^{3}He, α) and Fig. 6 for typical (p, d) spectra.[16] The comparison between the 20 and 40° (p, d) spectra illustrates the idea that the direct reaction components in the spectra become less significant with increasing reaction angle. For angles as large as 60°, the direct com-

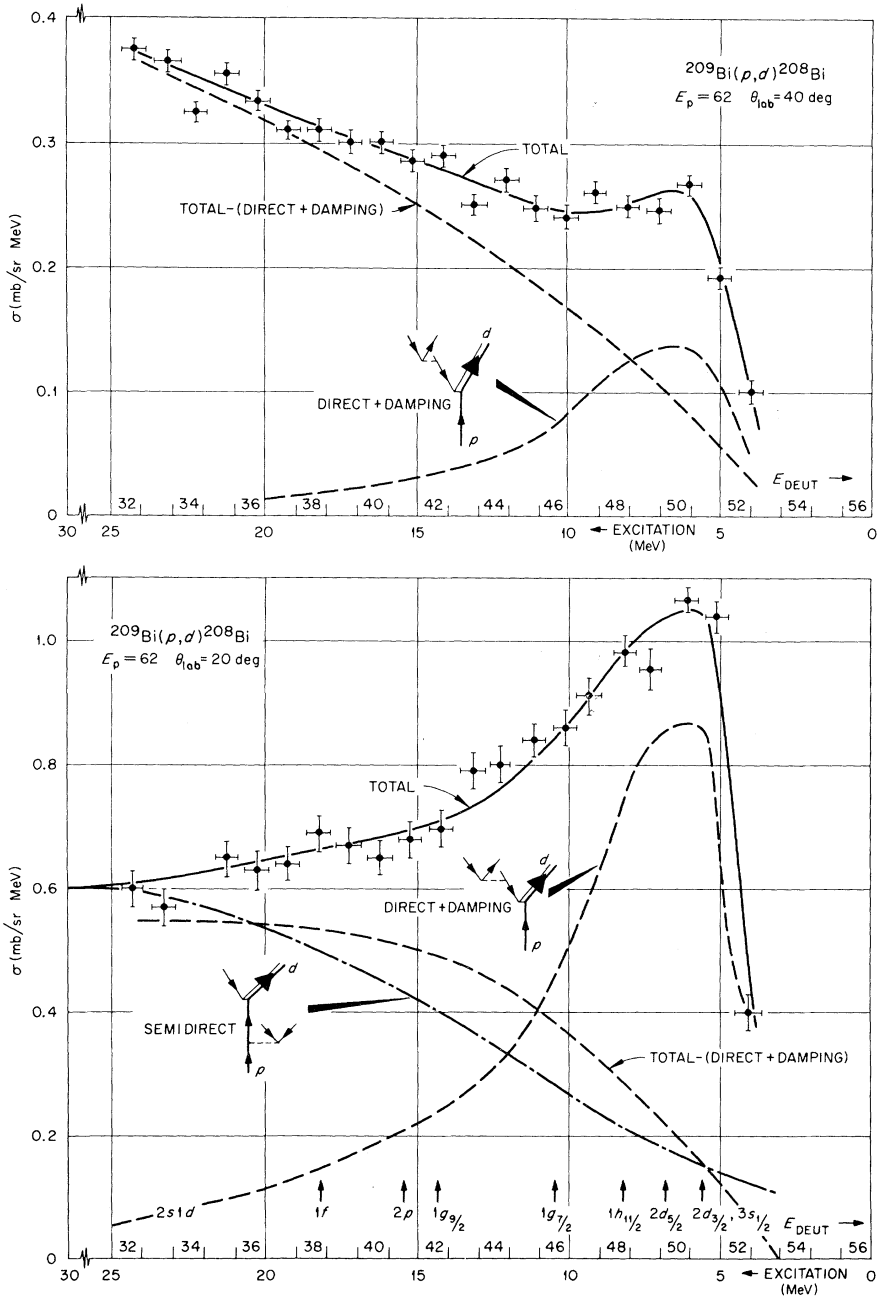

FIG. 6. Data (Ref. 16) and calculations (see text) for the resonance region of the deuteron continuum in the ^{209}Bi(p, d) reaction.

ponents are nearly imperceptible. In Fig. 3 the large contribution to the total resonance from the $1h_{11/2}$ hole component is shown. Part of the asymmetry of the total resonance, as well as its finite extent, can be understood by the energy dependence of the spreading width (or level density). Note, for example, the $1g_{9/2}$ hole component also shown in Fig. 3. The large spreading width (due to higher excitation energy) of this hole component makes it almost invisible in the experimental spectrum, forming only a shoulder on the dominant $h_{11/2}$ component. The still higher energy-hole components are not discernible against the strong background (indirect reaction) continuum.

The empirically determined spreading parameter required to fit the data is $s = 0.05$ MeV^{-1} with an uncertainty judged to be ± 0.02 MeV^{-1}. The single-particle j-state density in ^{208}Pb, based upon known neutron particle and hole states ($N = 82-126$) with 3-MeV shell gaps, is $g = 1.2$ MeV^{-1}. Thus, from g and s one can derive from Eq. (4) the effective interaction $M \approx 100$ keV, a value typical[17] of two-body matrix elements in the lead region. The uncertainty in the individual E_j in Table I is difficult to estimate except for the $E_{h_{11/2}}$ which is probably accurate to ± 1 MeV.

B. Continuum region

In Sec. III A it was found that the direct neutron pickup reaction estimates fell far short of explaining continuum cross section. The difference between the measured and direct cross sections are shown in Fig. 6 for the (p, d) reaction. In Sec. II D we assumed an average cross section $\langle\sigma(\theta)\rangle$ for the semidirect (i.e., two-step) excitation of a 2h-1p state and then proceeded to estimate [Eq. (7c)] the differential continuum, $\sigma^{(2)}(\theta, E)$, implied by the same density of states which determine the damping of the hole states. From Eq. (7c) it would appear that the $\sigma^{(2)}(\theta, E)$ would diverge with increasing excitation energy. However, the divergence of the $\rho(E')$ in the numerator of Eq. (7c) is checked by the divergence of the spreading width $\Gamma(E')$ implied in the denominator of the $R(E, E')$ function [see Eq. (6)]. To see this we make the plausible assumption that the damping of an n_p-particle-n_h-hole state is simply the incoherent sum of the individual particle and hole damping, each nucleon sharing $1/(n_p + n_h)$ fraction of the total excitation energy. In other words, if Eq. (4b) is valid for the damping of a 1h or 1p state, then we have the general expression for an n_hh + n_pp system,

$$\Gamma(E) = s(n_p + n_h)[E/(n_p + n_h)]^2 = s_n E^2 \ , \qquad (8)$$

where $s_n = s/(n_p + n_h)$. It is clear from Eq. (8) that not only will resonances disappear at very large excitation energies, but at a given excitation energy, they will become sharp as the complexity of nucleon participation in the state increases. These properties, of course, were expected from general observation of nuclear spectra.

We can now understand why the high excitation reaction continuum spectra are expected to be a slowly varying function of energy: the variation in the density of states is mostly compensated by the damping of the same states. Applying the same parameters, $g = 1.2$ MeV^{-1} and $s = 0.05$ MeV^{-1}, from the damping of the hole states in Sec. III A to Eq. (7c), we get the semidirect continuum curve shown in Fig. 6. This background curve can be seen to be similar to the one deduced from taking the difference between the measured cross section and the direct (DWBA) curve. We have here arbitrarily adjusted the average two-step cross section:

$$\langle\sigma'(20°)\rangle = 0.0050 \text{ mb/sr}.$$

It is encouraging that relatively large differential continuum cross sections can be generated from very small two-step reaction cross sections. In a later publication we hope to present an estimate of $\sigma'(\theta)$ based upon coupled-channel calculations in order to determine a realistic quantitative estimate for $\sigma^{(2)}(\theta, E)$.

IV. INELASTIC SCATTERING SPECTRA

In general, sum rules in nuclear reactions imply transition rates associated with certain regions of the total configuration space. From this viewpoint, all types of reactions have sum rules which apply to various configurations reached in the product nucleus. In the previous sections we discussed the hole state configurations. It is well known that the energy-weighted sum rules for collective excitations are far from being exhausted by discrete levels in an excited nucleus. Therefore, it is feasible that the excitation of many collective states (or resonances) are an important, if not dominant, mode by which the high particle-energy inelastic scattering continuum is formed. If this is true, the experimental inelastic scattering continuum will not necessarily be smooth, but it could have resonance-like structure whose shape is in part determined by the same damping mechanism which determined the shape of the pickup spectra discussed previously. A closer analogy results if we consider a specific 1p-1h component of the quadrupole vibration as is shown in Fig. 7. It can be seen that the inner shell $2d_{5/2}$ hole state is a component to the $(2g_{9/2}2d^{-1}{}_{5/2})$ configuration vector of the 2^+ vibration. Thus, a

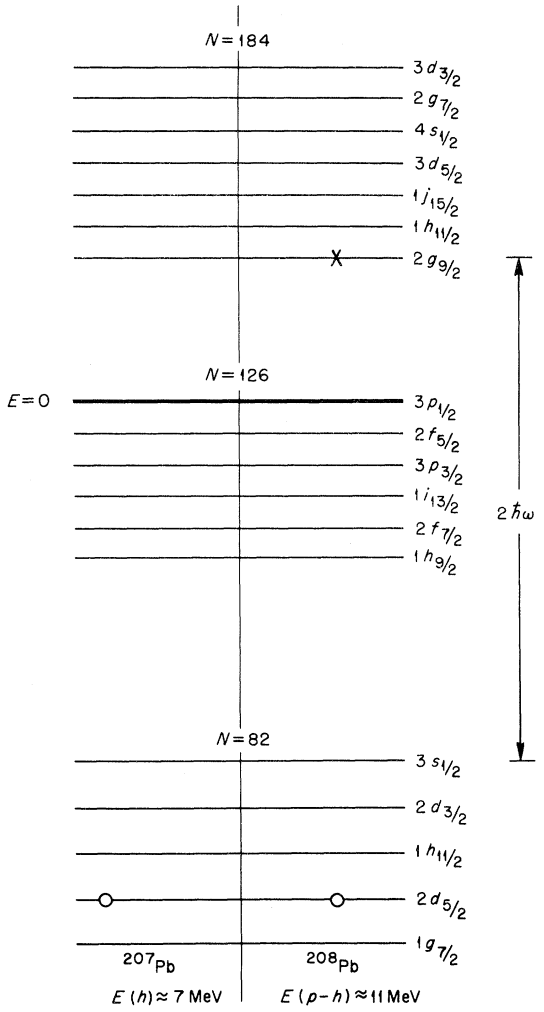

FIG. 7. Single-particle level diagram for ^{208}Pb; the inner shell hole states such as $2d_{5/2}$ are seen to be components in the particle-hole vibration, such as the 11-MeV quadrupole resonance in ^{208}Pb (Ref. 2).

damping of the 1p-1h vibration into 2p-2h states is expected (in this example) to take place via the spreading of the hole state previously discussed.

Only those 2p-2h states which can be reached by scattering diagrams like those in Fig. 4 are important to the damping process, and the density of these states are, of course, the same as the density of 2h-1p or 2p-1h states, each of which has the energy dependence in the equidistant spacing model given in Eq. (2). Thus, the energy dependence of the spreading width of giant vibrations is similar to that for the hole states. Applying Eq. (8) to the 1p-1h system, we get

$$\Gamma(E) = s_2 E^2 = \tfrac{1}{2} s E^2 \ , \tag{9}$$

where s is the same spreading parameter empirically determined in Sec. III: $s = 0.05$ MeV^{-1}. From Eq. (9) one gets $\Gamma = 4.6$ MeV for the well-known giant dipole resonance ($E = 13.4$ MeV) in ^{208}Pb; this estimate is consistent with the measured value, $\Gamma = 4.1$ MeV.[18] Since there is little information on the actual energies of most of the expected collective excitations in the continuum, no attempt will be made to calculate the direct or semidirect spectral components suggested in Fig. 5. We merely make the qualitative point that the strong energy dependence of the spreading width is nearly independent of J^π. Therefore, the observation of resonance structure at excitation energies far above the well-known electric dipole state would be precluded in a simple inelastic scattering experiment.

V. SUMMARY

We have attempted to show that one can better understand experimental reaction spectra by assuming that the high (particle) energy or lower excitation region of the nuclear continuum in a given reaction consists of at least two elements related to the nuclear spectroscopy of the more familiar discrete region of reaction spectra; namely, (1) simple configurations absorbing the complement of the same sum rules appropriate to well-known configurations in the discrete spectra and (2) configurations degenerate with (1) but having one degree higher complexity. The existence of configurations of type (2) distorts the reaction spectra by: (a) damping; i.e., mixing with and spreading states with configuration type (1) over several MeV excitation energy, and (b) indirect excitation; i.e., being semidirectly excited by two-step reaction mechanisms, thus forming a nonisotropic and energy-dependent continuum, $\sigma^{(2)}(\theta, E)$, background. Finally, we have compared in a meaningful way the damping width of a "hole" resonance in a pickup reaction with the width of a giant dipole resonance which might be excited in an inelastic scattering reaction.

The author is indebted to G. R. Satchler and R. L. Becker for many helpful discussions.

*Research sponsored by the U. S. Atomic Energy Commission under contract with the Union Carbide Corporation.

[1]M. Sakai and K. I. Kubo, Nucl. Phys. A185, 217 (1972).
[2]M. B. Lewis and F. E. Bertrand, Nucl. Phys. A196, 337 (1972); see also the review article by G. R. Satchler, to be published.
[3]O. Nathan and S. G. Nilsson, in *Alpha-, Beta-, and Gamma-Ray Spectroscopy*, edited by K. Siegbahn (North-Holland, Amsterdam, 1965), Vol. I, pp. 640, 641.
[4]J. J. Griffin, Phys. Rev. Lett. 17, 478 (1966); a list of subsequent papers on this subject may be found in C. K. Cline, Nucl. Phys. A193, 417 (1972).
[5]G. Chenevert, Ph.D. thesis, 1969, University of Michigan (unpublished), available through University Microfilms, Inc., Ann Arbor, Michigan.
[6]G. R. Satchler, W. C. Parkinson, and D. L. Hendrie, Phys. Rev. 187, 1491 (1969).
[7]This viewpoint is the basis of "doorway state" theory developed by R. Block and H. Feshbach, Ann. Phys. (N.Y.) 23, 47 (1963).
[8]L. R. Petersen, Bull. Am. Phys. Soc. 12, 667 (1967).
[9]T. Ericson, Adv. Phys. 9, 425 (1960).
[10]A. Bohr and B. R. Mottelson, *Nuclear Structure* (Benjamin, New York, 1965), Vol. 1, p. 371.
[11]R. Y. Cusson, D. Kolb, and H. P. Trivedi, private communication.
[12]P. D. Kunz, private communication.
[13]W. C. Parkinson, D. L. Hendrie, H. H. Duhm, J. Mahoney, and J. Sandinos, Phys. Rev. 178, 1976 (1968).
[14]C. B. Fulmer, J. B. Ball, A. Scott, and M. L. Whiten, Phys. Rev. 181, 1565 (1969).
[15]F. Hinterberger, G. Mairle, U. Schmidt-Rohr, G. J. Wagner, and P. Turek, Nucl. Phys. A111, 265 (1968).
[16]F. E. Bertrand and R. W. Peelle, Oak Ridge National Laboratory Report No. ORNL-4638, 1971 (unpublished); Phys. Rev. C 8, 1045 (1973).
[17]T. T. S. Kuo, private communication; A. Heusler and P. von Brentano, Ann. Phys. (N.Y.) 75, 381 (1973).
[18]H. Beil, R. Bergere, P. Carlos, and A. Veyssier, C. R. Acad. Sci. (Paris) 269B, 216 (1969).